Forest Ecology and Management 365 (2016) 137–151

Contents lists available at ScienceDirect

Forest Ecology and Management

journal homepage: www.elsevier.com/locate/foreco

Spatial and temporal trends of drought effects in a heterogeneous semi-arid forest ecosystem

Timothy J. Assal [a,b,*], Patrick J. Anderson [a], Jason Sibold [c]

[a] U.S. Geological Survey (USGS), Fort Collins Science Center, 2150 Centre Avenue, Fort Collins, CO 80526, USA
[b] Graduate Degree Program in Ecology, Colorado State University, 1401 Campus Delivery, Fort Collins, CO 80523, USA
[c] Department of Anthropology, Colorado State University, 1787 Campus Delivery, Fort Collins, CO 80523, USA

ARTICLE INFO

Article history:
Received 24 September 2015
Received in revised form 16 January 2016
Accepted 17 January 2016

Keywords:
Landsat time-series
Temporal trend analysis
Drought effects
Forest-shrubland ecotone
Rocky Mountain forests

ABSTRACT

Drought has long been recognized as a driving mechanism in the forests of western North America and drought-induced mortality has been documented across genera in recent years. Given the frequency of these events are expected to increase in the future, understanding patterns of mortality and plant response to severe drought is important to resource managers. Drought can affect the functional, physiological, structural, and demographic properties of forest ecosystems. Remote sensing studies have documented changes in forest properties due to direct and indirect effects of drought; however, few studies have addressed this at local scales needed to characterize highly heterogeneous ecosystems in the forest-shrubland ecotone. We analyzed a 22-year Landsat time series (1985–2012) to determine changes in forest in an area that experienced a relatively dry decade punctuated by two years of extreme drought. We assessed the relationship between several vegetation indices and field measured characteristics (e.g. plant area index and canopy gap fraction) and applied these indices to trend analysis to uncover the location, direction and timing of change. Finally, we assessed the interaction of climate and topography by forest functional type. The Normalized Difference Moisture Index (NDMI), a measure of canopy water content, had the strongest correlation with short-term field measures of plant area index ($R^2 = 0.64$) and canopy gap fraction ($R^2 = 0.65$). Over the entire time period, 25% of the forested area experienced a significant (p-value < 0.05) negative trend in NDMI, compared to less than 10% in a positive trend. Coniferous forests were more likely to be associated with a negative NDMI trend than deciduous forest. Forests on southern aspects were least likely to exhibit a negative trend while north aspects were most prevalent. Field plots with a negative trend had a lower live density, and higher amounts of standing dead and down trees compared to plots with no trend. Our analysis identifies spatially explicit patterns of long-term trends anchored with ground based evidence to highlight areas of forest that are resistant, persistent or vulnerable to severe drought. The results provide a long-term perspective for the resource management of this area and can be applied to similar ecosystems throughout western North America.

1. Introduction

Climate shapes vegetation patterns through the balance between energy supply, moisture and the seasonal timing of the two (Stephenson, 1990). In this way, the climate of a region exerts top-down control on ecosystem pattern and process. Ecosystem disturbance, in particular large, infrequent disturbances (Turner and Dale, 1998), are also recognized as a key mechanism of landscape pattern in forests due to the enduring legacies of physical and biological structure that result from these events (Foster et al., 1998). However, disturbance also operates at less conspicuous scales and the range of disturbance impacts are best thought of along a continuum (Sousa, 1984), as legacies can persist at some level regardless of the size or frequency of the disturbance (Turner et al., 1998). Drought and desiccation stress are forms of ecosystem disturbance (Sousa, 1984), yet the spatial and temporal complexity of drought renders identification and quantification very difficult (Vicente-Serrano, 2007).

In the early 2000s, over half of the coterminous United States experienced moderate to severe drought conditions and record breaking precipitation deficits throughout the western part of the country (Cook et al., 2004). These events brought attention to drought vulnerability in semi-arid forests of western North America. Portions of the intermountain west also experienced severe to

* Corresponding author at: USGS, Fort Collins Science Center, Fort Collins, CO 80526, USA.
E-mail address: assalt@usgs.gov (T.J. Assal).

http://dx.doi.org/10.1016/j.foreco.2016.01.017
0378-1127/Published by Elsevier B.V.

extreme drought in 2012 (NOAA, 2012). Severe drought in the early part of the last decade has been identified as the driver of tree stress, dieback and mortality across diverse forest types (Allen et al., 2010; Breshears et al., 2005; Gitlin et al., 2006; Michaelian et al., 2011). These events also contribute to flammability of fuels and decreased snowpack, resulting in longer fire seasons (Littell et al., 2009; Westerling et al., 2006).

The physiological drivers of tree mortality are complex (McDowell et al., 2008) and drought produces a gradient of effects on coniferous and deciduous forests in western North America. Drought can induce direct or indirect tree mortality, however, less conspicuous effects such as loss of productivity can accompany drought as well (Hogg et al., 2008). Forest response to drought is likely dependent on the spatial pattern of forest structure and function (Baguskas et al., 2014; Hope et al., 2014), and the duration of the drought is a key element in plant response (Dorman et al., 2013). Water stress can lead to an increase in plant respiration (Jones and Vaughan, 2010), and plants cope with drought via stomatal closure and reduced leaf area index (LAI) (Hope et al., 2014). A reduction in leaf area leads to a lower photosynthetic capacity and a change in canopy structure. Collectively, these responses result in a decrease in chlorophyll and water content of plant leaves (Jones and Vaughan, 2010). Drought stress is often coupled with multiple, interacting factors (Allen et al., 2010), and lag effects of drought may lead to tree dieback and mortality several years after the drought event (Bigler et al., 2007).

Multiple studies have documented an increase in mortality rates of coniferous species throughout the western United States over the later part of the 20th century (Allen and Breshears, 1998; Breshears et al., 2005; van Mantgem et al., 2009). Increases in mortality rates have been reported across ecosystem type and elevation, among dominant genera and tree size, and at sites with diverse fire histories (Gitlin et al., 2006; van Mantgem et al., 2009). All of these mortality events were driven by increased water deficit associated with drought, but secondary agents such as bark beetle outbreaks have also contributed to conifer mortality in some areas (Bentz et al., 2010; van Mantgem et al., 2009). The dominant deciduous tree in western North American, quaking aspen (*Populus tremuloides*), may have an advantage over coniferous trees during periods of lower moisture due to its clonal root system. However, droughts of long durations are likely to affect the growth of both suckers and mature trees alike (Hessl and Graumlich, 2002). Severe drought in the boreal forest and parkland of western Canada resulted in a two-fold increase in stem mortality and a 30% decrease in regional stem growth in persistent trees (Hogg et al., 2008). Decrease in growth is the result of high levels of twig and branch dieback in the crowns of living trees and productivity is limited by carbon dioxide fixation imposed by leaf stomatal resistance during soil or atmospheric water deficits (Hogg et al., 2000). A phenomenon known as sudden aspen decline (SAD) has been documented in regional aspen forests (Worrall et al., 2008). Rapid and sudden onset of mortality is primarily caused by high temperatures, acute drought and secondary biotic agents (Worrall et al., 2008).

Disturbance alters ecosystem structure by both abrupt, obvious change and through gradual, slow change over some period of time (Assal et al., 2014). Remote sensing offers a powerful medium to capture the pre and post disturbance landscape and detect changes that might not be readily observed, such as drought stress. Spatial, temporal and spectral scales are an important consideration when using remote sensing in ecosystem disturbance studies. Two common multispectral remote sensing platforms used in drought studies are the Moderate Resolution Imaging Spectroradiometer (MODIS) (Abbas et al., 2014; Bastos et al., 2014; Hope et al., 2014) and the Landsat satellites (Huang and Anderegg, 2012; Maselli, 2004; Vogelmann et al., 2009; Volcani et al., 2005). Both platforms are well suited to study ecosystem dynamics at regional scales given the large coverage area per scene. However, subtle changes in forest structure and productivity are difficult to detect with satellite derived observations (Deshayes et al., 2006). Therefore, drought studies require a long-term series of observations, which makes the high temporal resolution of these satellites well suited for this application. Although MODIS has a high-temporal resolution (16-day composite product compared to 16-day revisit time for Landsat), the lower spatial resolution (250–500 m compared to 30 m) precludes its use in highly heterogeneous forest-shrubland ecotones. Trend analysis utilizing time-series of Landsat data is useful to identify, monitor, and assess both abrupt and subtle forest change (Czerwinski et al., 2014; Dorman et al., 2013; Kennedy et al., 2010; Vogelmann et al., 2009).

Forest canopy reflectance is influenced by several biophysical parameters including crown closure, canopy and branch architecture, LAI, the chlorophyll and water content of leaves as well as the understory and exposed soil properties of the stand (Deshayes et al., 2006). Multispectral satellites have spectral bands spanning the visible and infrared wavelengths that can be combined into vegetation indices that are sensitive to differences in these biophysical parameters (Jones and Vaughan, 2010). Living vegetation absorbs radiation in portions of the visible wavelengths and reflects in the near-infrared (NIR); whereas radiation in the shortwave-infrared (SWIR) is absorbed by water content of leaves (Jones and Vaughan, 2010). The NIR and SWIR are sensitive to variations in LAI and the SWIR band is sensitive to water stress during periods of drought (Deshayes et al., 2006). Numerous spectral vegetation indices have been used in disturbance and drought studies, many of which utilize the NIR and/or the SWIR bands. The Normalized Difference Vegetation Index (NDVI) is the most widely used vegetation index to document and monitor drought and related impacts in forests (Breshears et al., 2005; Carreiras et al., 2006; DeRose et al., 2011; Lloret et al., 2007; Maselli, 2004; Volcani et al., 2005; Weiss et al., 2004). However, other vegetation indices have utility in disturbance related vegetation dynamics including the Enhanced Vegetation Index (EVI) (Hope et al., 2014; Tüshaus et al., 2014), the Normalized Difference Moisture Index (NDMI) (Goodwin et al., 2008; Meddens et al., 2013), the soil adjusted vegetation index (SAVI) (Tüshaus et al., 2014), and the Tasseled Cap (Czerwinski et al., 2014).

We sought to quantify the spatial and temporal effects of drought in a semi-arid mixed forest ecosystem that is expected to be vulnerable to drought stress and climate change. The effects of climate change and variability are expected to be most rapid and extreme at ecotones, especially in semi-arid forests (Allen and Breshears, 1998; Gosz, 1992). An understanding of the link between climate variability and tree mortality for species near ecotones is an important focus of current research (Kulakowski et al., 2013). Ecotones are important barometers of climate change (NEON, 2000) and stress, dieback and mortality are expected to accompany severe drought in this arid landscape. Recent studies (Crookston et al., 2010; Rehfeldt et al., 2009) predict the current climate profile for several prominent tree species (e.g. aspen, subalpine fir and lodgepole pine) will be greatly limited or no longer present in isolated forests of the Rocky Mountains over the course of the next century. However, regional climate can be influenced by local topography, a concept known as topoclimate (Thornthwaite, 1953). Slope, aspect and other topographic features influence air temperature, water balance, radiation, snowmelt patterns and wind exposure (Dobrowski, 2011) which amplify the effects of drought, particularly in arid landscapes.

The use of temporal remotely sensed data has been effective in monitoring drought induced changes in forests and woodlands (Maselli, 2004; Vogelmann et al., 2012). A primary challenge in spectral change analysis is to segregate long-term vegetation

change from interannual phenology differences in response to climate variability. We hypothesize that the ecological consequences of drought create a landscape mosaic of drought effects and that trend analysis of vegetation indices can be used to document the distribution and magnitude of a gradient of effects (Lloret et al., 2007). The gradient of drought effects include demographic (i.e. tree mortality), structural (i.e. crown partial dieback), functional (i.e. reduction in leaf area), and physiological (i.e. temporary/permanent reduction in photosynthetic activity) properties of the forest ecosystem that result in different spectral trajectories. This study was undertaken because little is known about baseline condition in the forest, and how climate, in particular drought, affects this topographically complex ecosystem. Finally, we are interested in providing resource managers with a long-term perspective of the forest dynamics of this ecosystem with respect to variability in precipitation patterns.

Our research objectives were to:

(1) Identify an appropriate vegetation index for use in temporal trend analysis based on the relationship with field measured estimates of vegetation traits,
(2) Analyze the spatial location, trend direction, and timing of spectral change by forest type, and
(3) Determine the correlative relationship between spectral change and tree mortality, and assess this relationship with topographic features.

2. Methods

2.1. Study area

Our study area is located in the southern part of the Wyoming Basin ecoregion, spanning parts of southwestern Wyoming, northwestern Colorado and northeastern Utah (Fig. 1). Several prominent ridges form a transition zone between basins and mountainous areas (Knight, 1994), where several species of trees are found at the xeric fringes of their respective ranges. Forests dominated by aspen (*Populus tremuloides*) and several coniferous species (subalpine fir (*Abies lasiocarpa*), lodgepole pine (*Pinus contorta*), and Douglas-fir (*Pseudotsuga menziesii*)) occur as relatively small patches on moist sites in a matrix of sagebrush steppe (*Artemisia tridentata* spp. *vaseyana*) or mixed-species shrublands. Scattered juniper (*Juniperus communis var. depressa*) and limber pine (*Pinus flexilis*) woodlands, distinct from the montane conifer forest, are found on rocky slopes at lower elevations and small patches of manzanita (*Arctostaphylos patula*) are found in the southern part of the study area. Most of the area is under the jurisdiction of the U.S. Bureau of Land Management, interspersed with small parcels of State and private land. The area has a midlatitude steppe climate with a substantial portion of the annual precipitation occurring as snow. Dominant land uses include livestock grazing, energy extraction and recreation. Multiple State and Federal agencies, along with the Wyoming Landscape Conservation Initiative (wlci.gov), have identified this region as a priority area for conservation. The area provides important habitat for many wildlife species including big game, migratory and resident birds, as well as domestic livestock. Management has sought to rejuvenate decadent aspen stands and reduce conifer expansion in successional aspen stands through prescribed fire and mechanical thinning. Drought related mortality of aspen is a concern in western North America (Worrall et al., 2008) and lack of aspen regeneration due to high rates of herbivory is a concern in the study area.

2.2. Drought index calculation

To understand the effects of drought at a local level, we needed to develop a localized index of drought severity. The most widely used drought index, the standardized precipitation index (SPI) (Vicente-Serrano, 2007), was used to quantify surface water deficit and surplus. We used the SPI instead of the regional Palmer Drought Severity Index to capture local differences in annual precipitation of the relatively small and isolated study area. The SPI indicates the number of standard deviations that precipitation deviates from the long-term mean during the measured period (Vicente-Serrano, 2007). The majority of the precipitation in the study area is received in the form of snow. The flexibility of the SPI enabled us to calculate a 12-month duration equivalent to the water year (Oct–Sept) between 1975 and 2014. We obtained 4 km^2 SPI data from the Western Regional Climate Center (http://www.wrcc.dri.edu; accessed 15 February 2015) and calculated the water year mean for a 50 km^2 area that encompasses the forested ridges of the study area.

2.3. Satellite data

The growing season in the study area is short, with snow possible in mid-June and leaf senescence by late September. To select a consistent window of peak greenness, we calculated the average growing season phenology (2000–2012) of the forested portion of the study area using MODIS NDVI 16-day composite data (MOD13Q1). Predominantly cloud-free Landsat images were selected between July 01 and September 06 (day of year 182–249 in non-leap years). A total of 24 Landsat Thematic Mapper (TM), Enhanced Thematic Mapper Plus (ETM+), and Operational Land Imager (OLI) images (path 36, row 32) were acquired for analysis from the USGS EarthExplorer Archive (USGS, 2014) between 1985 and 2014 (Table 1). The imagery was processed to surface reflectance using the Landsat Ecosystem Disturbance Adaptive Processing System (LEDAPS) (Masek et al., 2006) which has been successfully used in other ecosystem change studies (McManus et al., 2012). We used the LEDAPS quality mask layer to identify pixels with clouds, cloud shadows and other unacceptable pixels that were removed from the analysis. We calculated several vegetation indices (Table 2) using the Landsat 8 OLI imagery to explore relationships between each vegetation index and the field data. We then applied the index that best explained variation in the short-term field data (see Section 3.3) to the Landsat time series.

In order to extend the time series beyond 2011, it was necessary to use several Landsat ETM+ images with gaps due to the scan-line corrector problem that occurred in 2003 (Chander et al., 2009). Landsat TM data are not available after the growing season of 2011 and we chose not to incorporate Landsat OLI data (available beginning in June 2013) given the wavelengths of several key bands are different from earlier Landsat satellites, and a reliable calibration process has not yet been documented. We obtained six ETM+ scenes from 2012, 2013 and 2014. We sought to connect pixels through time (z) and not space (x, y), and therefore a traditional image normalization technique would not be appropriate. We conducted a sensitivity analysis between annual images using our field plot locations ($n = 52$) and several vegetation indices to evaluate the annual phenological stability between dates. The Pearson's correlation coefficient for each index in each of the three years was $\geqslant 0.85$. However, we only retained the data from 2012 as the available images were consecutive (Aug 03 and Aug 19) and the field points were highly related (Pearson's correlation coefficient NDMI = 0.95, NDVI = 0.94). A composite 2012 image was created using the earlier image as the primary value and the later image

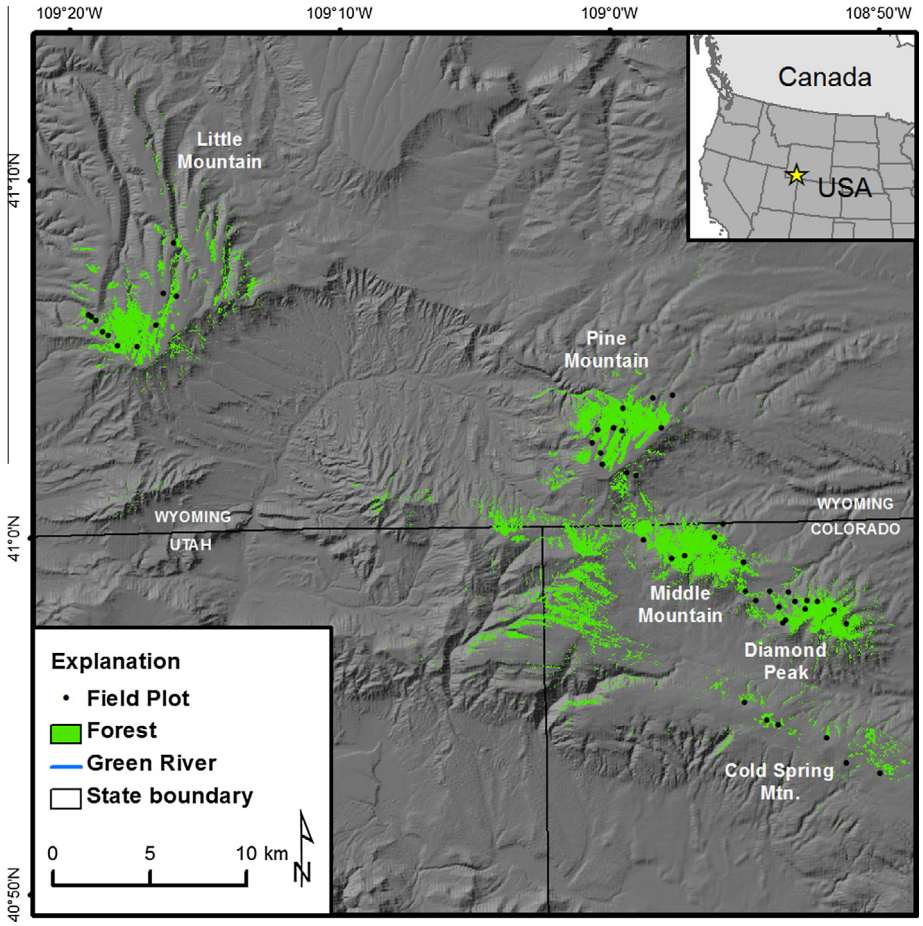

Fig. 1. Location and extent of forest and field plots in the study area.

Table 1
Acquisition dates of Landsat scenes used in the analysis (path 36, row 32). Note, the OLI image was used to establish the relationship between field measured data and vegetation indices and was not used in the trend analysis. TM = Thematic Mapper, ETM+ = Enhanced Thematic Mapper Plus, and OLI = Operational Land Imager.

Acquisition date (year-month-day)	Sensor
19850811	TM
19880724	TM
19910903	TM
19920828	TM
19930823	TM
19940709	TM
19950728	TM
19960831	TM
19970701	TM
19980805	TM
20000725	TM
20010829	TM
20020731	TM
20030819	TM
20040906	TM
20050905	TM
20070830	TM
20080731	TM
20090819	TM
20100705	TM
20110809	TM
20120803	ETM+
20120819	ETM+
20140902	OLI

was used to overwrite pixels with no data. We also obtained a Landsat OLI scene to evaluate the relationship between field data and spectral vegetation indices. The OLI image was acquired several days before our field collection effort in 2014.

Table 2
Spectral indices calculated from the Landsat OLI reflectance data; NDVI (Normalized Difference Vegetation Index), NDMI (Normalized Difference Moisture Index), EVI (Enhanced Vegetation Index), and SAVI (Soil Adjusted Vegetation Index). EVI constants: G (gain factor) = 2.5, L (canopy background adjustment factor) = 1, C1 (atmospheric constant) = 6, C2 (atmospheric constant) = 7.5. SAVI constants: L (soil adjustment factor) = 0.5 (intermediate vegetation density).

Spectral Index	Equation	Source
NDVI	NDVI = (near-infrared – red)/(near-infrared + red)	Rousse et al. (1974)
NDMI[a]	NDMI = (near-infrared – mid-infrared)/(near-infrared + mid-infrared)	Wilson and Sader (2002)
EVI	EVI = G * (near-infrared – red)/(near-infrared + C1 * red – C2 * blue + L)	Huete et al. (2002)
SAVI	SAVI = (near-infrared – red)/(near-infrared + red) * (1 + L)	Huete (1988)

[a] Note: the same band combinations used in NDMI were first formulated by Hardisky et al. (1983) and referred to as the Normalized Difference Infrared Index (NDII).

2.4. Field measurements

We conducted a preliminary investigation to identify areas of change and stability over time using NDVI from several years (mid-90s, early 2000s, and 2010). With a focus on description rather than prediction, we employed a purposive field sampling approach

to allow rapid collection of data to describe a range of conditions across the study area (Meigs et al., 2011). We identified 52 plots (Fig. 1) evenly distributed in coniferous and deciduous forests on each of the major forested ridges in the study area. We avoided areas with substantial anthropogenic activity (e.g. logging, recreational sites, roads, trails, stock tanks, etc.) or fire occurrence since 1984 (Eidenshink et al., 2007).

In 2013, we collected plot level measurements to assess tree density, species composition and structure, and tree mortality (Meigs et al., 2011). We consider these measurements long-term data as we presume they reflect conditions for a number of years prior to measurement since there were no major disturbances in each plot. Each plot was located at the center of a Landsat pixel (30×30 m) using a sub-meter GPS unit (Trimble GeoXT). Three, 15 m belt transects were established from the plot center at 0° (true north), 120°, and 240° with a variable width of two or four meters. In each transect we quantified live and dead tree basal area for all standing tree species greater than 2 meters in height. We noted canopy dieback, bark damage, and presence of cankers or insect damage. We also counted dead, down trees that were likely rooted within each transect (Meigs et al., 2011) and assigned a bark decay class (1–5) according to USFS Forest Inventory and Analysis standards. In this analysis, we retain the lowest decay classes (1–3) as they were most likely alive in recent decades.

In 2014 we revisited the field plots to measure canopy condition via in situ plant area index (PAI) and canopy gap fraction (CGF). We consider these short-term data as they likely reflect recent conditions at each plot. We used a hand-held CID-110 Plant Canopy Imager instrument (CID Bio-Science, Inc.) to collect hemispherical (fish-eye) plant canopy images to estimate PAI and CGF. The process relies on the gap-fraction inversion procedure (Campbell and Norman, 1989) to measure radiation transmission through the canopy (Martens et al., 1993). The instrument contains a self-leveling PENTAX lens that enabled images to be collected looking vertically upward beneath the canopy at approximately one meter above the ground. Measurements were performed under a range of sky conditions, as the study area rarely experiences prolonged overcast conditions (Pfeifer et al., 2012). Exposure, color, and contrast settings were manually adjusted to maximize the contrast between the sky and canopy. A sampling grid was established within each 30×30 m plot and nine photo points were collected (Fig. 2) for 43 of the 52 plots (due to equipment issues). The images were classified into sky and plant components using CID software and PAI and CGF were averaged for each plot. We use the term plant area index instead of leaf area index because this measurement includes stems and branches (Pfeifer et al., 2012). We opted not to subtract an estimated stem-area index because preliminary results indicated the PAI was sensitive to mortality levels between plots.

2.5. Statistical analysis of vegetation indices

We used a generalized linear model (GLM, Gaussian distribution, Identity link function) to evaluate the relationship between field and satellite data. Our goal was to identify the vegetation index with the strongest relationship to field data, not create a spatially explicit model of forest characteristics (e.g. PAI). We found the short-term data had the strongest relationship with that year's satellite data (e.g. 2014 field data with 2014 satellite data). This was expected as the Landsat OLI scene was acquired just days before the 2014 field campaign. The Canopy Gap Fraction data was log-transformed prior to the analysis to meet the assumptions of linear regression.

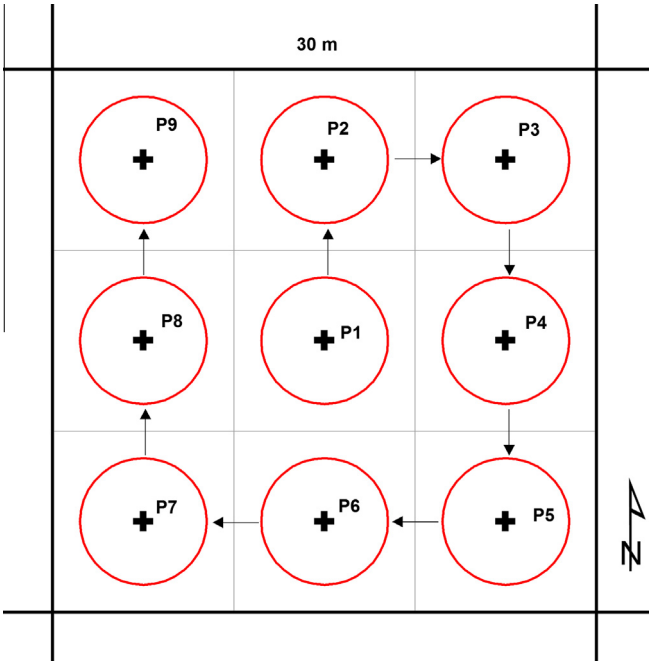

Fig. 2. Plot based sampling design for derivation of vegetation structure traits. Each hemispheric photo location is spaced approximately 10 m from the nearest photo point. The field of view of each hemispheric photo is shown (red circle) with an approximate radius of 3.5 m. (For interpretation of the references to colour in this figure legend, the reader is referred to the web version of this article.)

2.6. Temporal trend analysis

Trend analysis was implemented on a per-pixel basis using least-squares regression between the vegetation index (dependent variable) and time (explanatory variable) (McManus et al., 2012; Vogelmann et al., 2009). We evaluated trends for several time periods of n images and allowed one missing observation ($n - 1$) in each pixel stack. This allowed the use of several additional years of imagery with some cloud and cloud shadows present, while minimizing the potential for illegitimate trend detection (McManus et al., 2012). The slope and statistical significance of the linear regression in the selected vegetation index value (see Section 3.3) were evaluated using a Student's t-test at 95% confidence level for each geographic pixel (McManus et al., 2012). Significant temporal trends in NDMI may be interpreted as changes in vegetation condition, given the relationship between field and satellite data. Pixels identified with significant monotonic temporal trends (p = <0.05) were mapped as positive or negative change (Czerwinski et al., 2014). Trend analysis was conducted on all eligible (no more than one missing year due to clouds, cloud shadows, no fire) forested pixels in the study area over a range of time periods with at least ten observations.

2.7. Spatial analysis of NDMI trends

Positive and negative trends in NDMI between 1985 and 2012 were evaluated by dominant forest type. Using a 10 m raster map of forest cover and dominant forest type (e.g. deciduous vs. coniferous) (Assal et al., 2015) we resampled the data to 30 m using a nearest neighbor algorithm to retain small areas of forest along the shrubland margin. The map was developed from 2010 SPOT imagery so we added obvious omissions of small aspen stands documented in the field that were missing from the map due to recent mortality. Next, we evaluated trends in NDMI by elevation, slope and aspect to understand how trends were

distributed with respect to landscape position. Topographic variables were derived from a 10 m National Elevation Data Set including slope, and aspect. The relationship between elevation, slope and aspect was analyzed with respect to negative NDMI trend occurrence using a binomial generalized linear model. We selected a random sample of negative and no-trend observations for 10% of total observations of each class (McManus et al., 2012).

3. Results

3.1. Drought index

The SPI for the study area (Fig. 3) indicates high variability of precipitation over the last four decades with several distinct wet and dry periods. The majority of the 1980s were wet along with the mid to late 1990s. There was a multi-year drought in the late 1980s and early 1990s. The late 1990s had two extremely wet years (1995 and 1997), while 2002 and 2012 were classified as extreme drought years. With the exception of 2005 and 2011 (severely wet years), the area has been in a dry period since 2000.

3.2. Field data analysis

The field data results indicate that our sampling effort captured a wide range of plot-level mortality. We categorized the plots into deciduous or coniferous based on the majority of the total basal area. There were very few mixed plots, and the vast majority of plots contained 70% or more of the dominant forest type. Deciduous plots ranged from low (11%) to total (100%) mortality. Coniferous forest plots exhibited a similar range from 5% to 95% mortality. Mortality was not consistent for small, medium and large trees (stem DBH < 10 cm, 10–20 cm, and >20 cm, respectively). We encountered fewer small and medium dead conifer trees compared to the same size classes of deciduous trees (Fig. 4).

3.3. Relationship between field and satellite data

Field variables with the highest correlation with 2014 vegetation indices were PAI and CGF. NDMI had the strongest correlations with field measures, and was therefore selected as the appropriate metric and thus only those results are reported here. A significant positive linear relationship ($R^2 = 0.64$, $p < 0.0001$, $n = 43$) was found between field measured PAI and NDMI (Fig. 5a). A significant negative linear relationship ($R^2 = 0.65$, $p < 0.0001$, $n = 43$) was found between field measured CGF and NDMI (Fig. 5b). This result was expected as dense, canopies have greater moisture content than sparse, open canopies or canopies with high levels of mortality. The residuals of the linear regression models were spatially independent (PAI model, Moran's $I = -0.0428$, $p = 0.7$; CGF model, Moran's $I = -0.024$, $p = 0.9$). The 2013 long-term data (collected in 2013) did not exhibit as strong of a relationship with the satellite data. The highest correlation was live tree density with NDMI ($R^2 = 0.46$, $p < 0.0001$, $n = 52$). We also found a significant linear relationship between the short-term (2014) and long-term (2013) field data with the live tree density (strongest predictor) of PAI ($R^2 = 0.56$, $p < 0.0001$, $n = 43$) and CGF ($R^2 = 0.54$, $p < 0.0001$, $n = 43$).

3.4. Trend analysis of forest change

The results highlight the area of significant positive and negative trend for each time period with at least ten observations. The first time period, T_{1998} (1985–1998) highlights 1705 ha (27% of the forested area) with positive, increasing trends, and only 1.6% of the forested area (98 ha) experiencing negative trends (Table 3). These trends began to change starting with T_{2000} (1985–2000) as the amount of forested area with a positive trend decreased and the area of forest exhibiting negative trends began to increase. From T_{2000} to T_{2012} (1985–2012) the amount of forest in a significant negative trend increased every period from 160 ha (T_{2000}) to 1606 ha (T_{2012}). The negative trend was significant in over 25% of the forested area by 2012 (Table 3). The decrease in the area under the positive trend was not cumulative as with the negative trend. The positive trend decreased from T_{1998} to a low of only 2.7% of the area in a significant positive trend during the drought year of 2002 (172 ha). The amount of forest in a positive trend slowly increased to a similar area at the start of the dry period (2000), with just under 10% by 2012. Trends were not consistent across forest functional types over the full time period T_{2012} (1985–2012). A higher percentage of coniferous forest experienced significant positive trends compared to deciduous forest (Table 4), and both forest types had substantially more area associated with negative trends. Coniferous forest experienced a greater percentage of area with significant positive and negative trends for every time period since 2000 (Fig. 6).

3.5. Forest change trends and topography

Significant positive and negative NDMI trends were present across all of the forest ridges (Fig. 7). Our analysis confirmed that

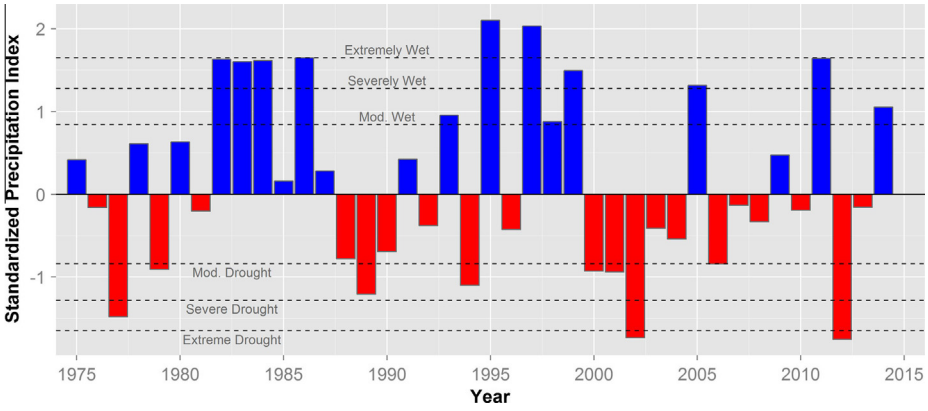

Fig. 3. Standardized precipitation index (SPI) for the study area between 1975 and 2014. The index was calculated over a 12-month period, equivalent to the water year (October of previous year through September of current year). The SPI is classified according to Agnew (2000); values between moderate drought and moderately wet indicate the range of normal conditions.

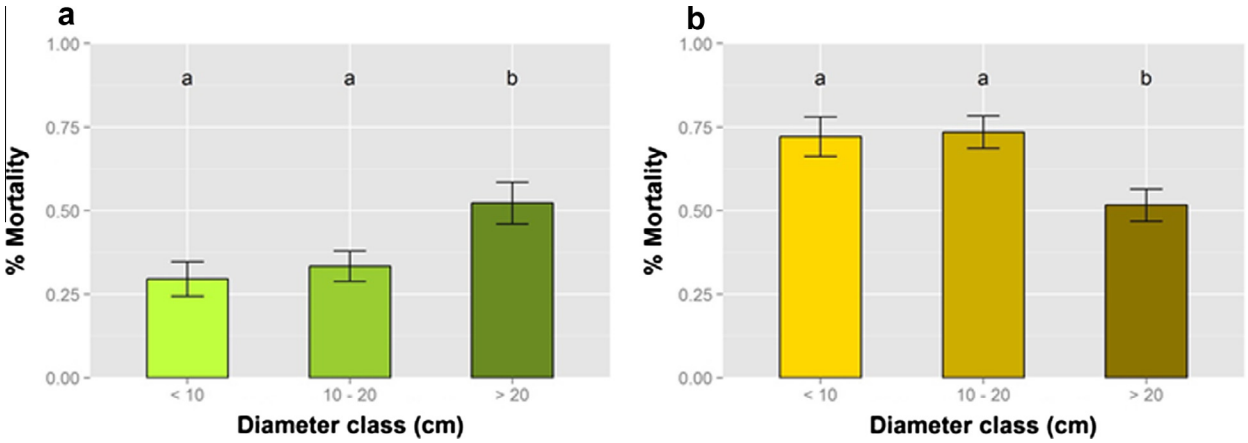

Fig. 4. (a) Relative mortality by tree size class in coniferous (n = 877) trees. (b) Relative mortality by tree size class in deciduous (n = 1162) trees. Relative mortality was estimated as the percent of dead and down trees by class per plot. Different letters in each figure denote significant differences at the 95% confidence level using a Tukey HSD test.

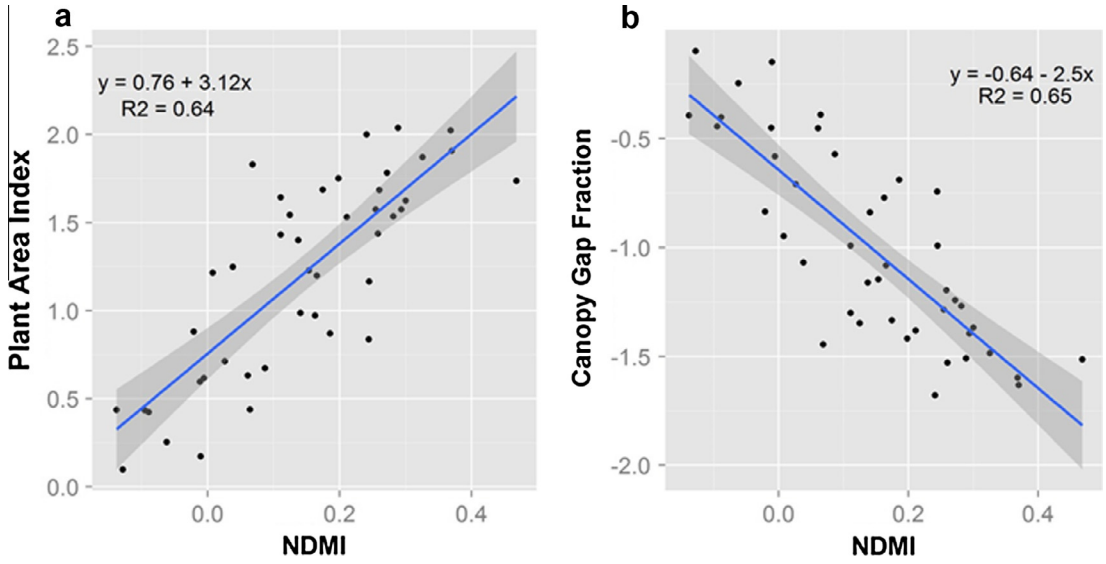

Fig. 5. (a) The relationship between field measured LAI/PAI and NDMI (n = 43). (b) The relationship between field measured Canopy Gap Fraction and NDMI (n = 43). Note that the y-axis is a log scale.

negative trends were not randomly distributed across the landscape with respect to topography. Forested areas at higher elevations were positively correlated with the frequency of detecting negative trends (Table 5). Forests on southern aspects (south, southeast and southwest) were least likely to exhibit a negative trend and north aspects were most likely to be associated with a negative trend. All aspects classes were significant, except for northeast aspects. We included forest type (deciduous or coniferous) in the GLM model, but it was not a significant explanatory variable and subsequently dropped. Positive trends with respect to topography were also analyzed, but very few variables were significant.

3.6. Ground based evidence of forest change trends

Field plots were identified a priori and therefore not evenly distributed with respect to trend significance or direction. A rigorous accuracy assessment or validation test could not be conducted; however, our data provide ground-based evidence that trends in NDMI reflect changing conditions in the forest. Nearly half of our field plots had a significant negative trend between 1985 and 2012. Of those plots, the magnitude of the slope provides a means to distinguish between mortality classes. An ANOVA with multi-comparison post-hoc Tukey's HSD test revealed significant differences between group means of the low and high mortality classes and the moderate and high mortality classes (Fig. 8a). Plots with a significant negative trend had a lower mean percentage of live trees compared to plots with no trend (p-value significant at the 0.1 level) (Fig. 8b). Plots with a negative trend had a significantly higher amount of standing dead and downed trees compared to plots without significant trends (p-value < 0.05) (Fig. 8c and d respectively).

The NDMI trajectories were extracted for each plot and analyzed to explore plot level trends over time. Figs. 9 and 10 are examples of field plots that exhibited negative NDMI trends from 1985 to 2012. Fig. 9 is a coniferous plot (dominated by Douglas-fir) with low plant area index (1.22), high canopy gap fraction (0.39), low live basal area (8.39 m^2/ha) and high plot mortality (68%). Pitch tubes were evident on many of the dead trees, indicating Douglas-fir beetle was responsible for the mortality at the site as exhibited with a sharp decline in NDMI beginning in 2005 (Fig. 9). Fig. 10 is an aspen stand with low plant area index

Table 3
Area of significant positive and negative NDMI trends for time series with greater than 10 observations. Trends reported have *p*-values that are significant at 0.05 or lower.

Time period	Observations (*n*)	Significant positive change		Significant negative change	
		Area (ha)	% of forest cover	Area (ha)	% of forest cover
1985–1998	10	1705	27	98	1.6
1985–2000	11	660	10.4	160	2.5
1985–2001	12	338	5.3	255	4.0
1985–2002	13	172	2.7	445	7.0
1985–2003	14	226	3.6	565	8.9
1985–2004	15	345	5.5	588	9.3
1985–2005	16	545	8.6	577	9.1
1985–2007	17	486	7.7	946	15.0
1985–2008	18	491	7.8	1127	17.8
1985–2009	19	567	9.0	1233	19.5
1985–2010	20	598	9.5	1291	20.4
1985–2011	21	720	11.4	1347	21.3
1985–2012	22	615	9.7	1606	25.4

Table 4
Summary of forest change between 1985 and 2012. The area and proportion of change for each group is compared to the total amount of that forest group.

Direction of change	Total change area (ha)	Functional group			
		Deciduous		Coniferous	
		Area (ha)	% of class	Area (ha)	% of class
Increase	615	205	7.1	410	11.9
Decrease	1606	474	16.5	1132	32.8

(0.43), a very open canopy (gap fraction = 0.64), low live basal area (12.8 m^2/ha), and very high mortality (81.5%). The NDMI trend (Fig. 10) provides a clear indication that the mortality was first instigated by drought in the early 2000s, and the stand never recovered. This is confirmed with the long-term field data as the plot had a much higher amount of total standing (live and dead) basal area (49.2 m^2/ha). Both of these plots began to decline around 2005, after a five year dry period centered on the 2002 drought (Fig. 3). Fig. 11 is an example of a plot that had a statistically significant positive trend over the study period. It was one of only two plots with a positive trend. The conifer dominated plot had relatively high plant area index (1.78), low canopy gap fraction (0.28), and high live basal area (34.2 m^2/ha) (Fig. 11). Fig. 12 is an example of a plot that did not have a statistically significant trend during the period of study. The deciduous plot is characterized by high plant area index (2.02), a low canopy gap fraction (0.2), and a high amount of live basal area (37.3 m^2/ha). The NDMI values are fairly high and stable throughout the period of study (Fig. 12) and track precipitation during two extremely wet years (1995 and 1997) (Fig. 3).

4. Discussion

Previous trend analysis studies have used multiple lines of evidence to support direction of change. Vogelmann et al. (2009) related areas of significant change to annual health aerial detection survey polygons and qualitative field sampling. Only a small portion of our study area was surveyed by aerial detection, and only during one year. Czerwinski et al. (2014) sampled a number of areas in the field with significant trends and qualitatively categorized each plot. McManus et al. (2012) correlated significant positive trends in NDVI to an increase in LAI based on a relationship with MODIS data across a regional scale. Our research establishes an empirical link between spatial differences in spectral reflectance and short-term field measured vegetation parameters such as plant area index and canopy gap fraction (Fig. 5). The statistically significant (95% confidence level) spectral trajectories (Czerwinski et al., 2014; McManus et al., 2012) provide a distinct level of certainty over the duration of the study period. Furthermore, our long-term field data (Fig. 4) provide a line of ground based evidence to interpret the spectral changes over time (Fig. 8). The framework we presented is suitable to retrospectively characterize the effects of drought in forest ecosystems over the last 30 years. The use of Landsat data is beneficial as the time series can be extended in the future once a calibration process is developed to incorporate Landsat 8 satellite (OLI sensor) data with TM and ETM + data.

4.1. Tree decline and mortality

Deciduous and coniferous forests are affected by different mechanisms of mortality. It is difficult to assign absolute causes of mortality without in-depth analysis (Vogelmann et al., 2009), however, we found evidence of causal agents on several field visits. Visible documentation of pine beetle (*Dendroctonus* spp.) activity was documented on dead trees in conifer stands in the form of pitch tubes (resin). Beetle caused mortality in lodgepole pine trees was likely caused by mountain pine beetle (*Dendroctonus ponderosae*), whereas Douglas-fir mortality was likely caused by the Douglas-fir beetle (*Dendroctonus pseudotsugae*). The Douglas-fir tussock moth (*Orgyia pseudotsugata*) and western spruce budworm (*Choristoneura occidentalis*) are defoliator species and may have also contributed to mortality in small Douglas-fir stands in the study area. However, we suspect the dominant cause of

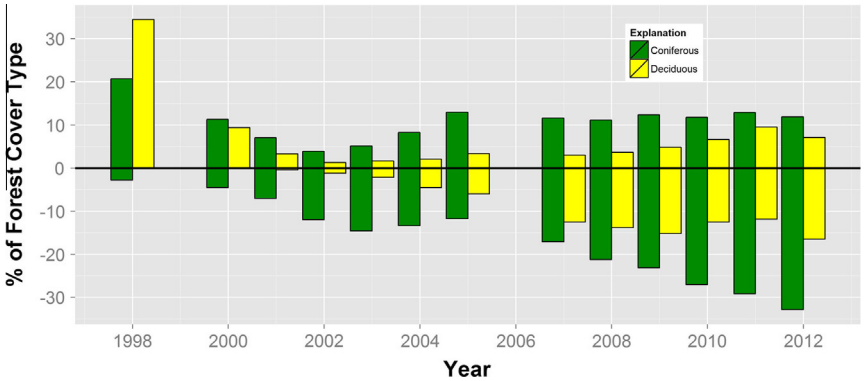

Fig. 6. The results of the forest change analysis for trends with 10 or more observations. Compare with Table 3. There was no imagery available for 1999 and 2006.

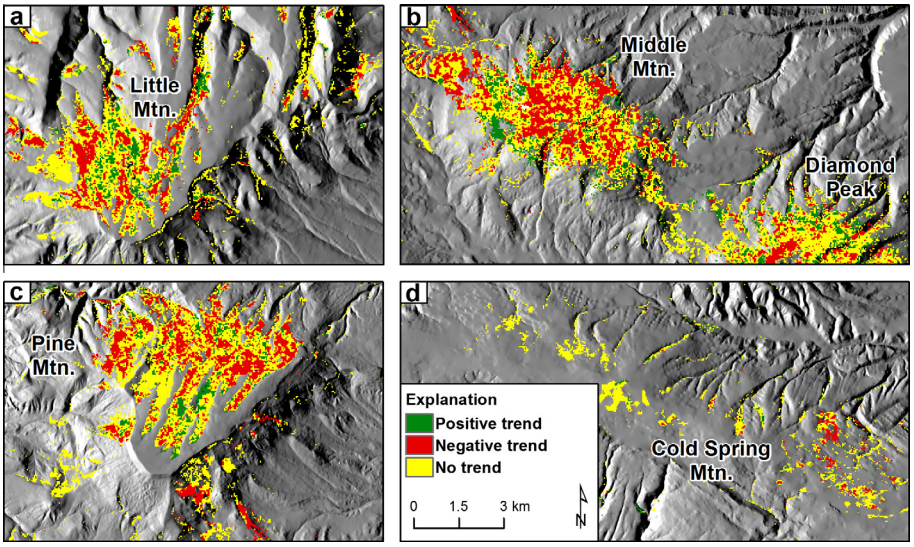

Fig. 7. Locations of forest with positive, negative and no (NDMI) trend over the full time period of study (1985–2012): (a) Little Mountain, (b) Middle Mountain and portions of Diamond Peak, (c) Pine Mountain, and (d) Cold Spring Mountain. Note, positive and negative trends are significant at the 95% confidence level. Each map panel is displayed at the same scale.

Table 5
Topographic coefficients from the generalized linear model (GLM) fit of significant negative trends between 1985 and 2012. The variable *Aspect* is an indicator variable (N is the reference class).

Predictor variable	Coefficient
(Intercept)	−8.22381[a]
Elevation	0.00286[a]
Slope	0.00234
Aspect	
N	NA
NE	−0.04581
E	−0.20159[a]
SE	−0.96975[a]
S	−1.27459[a]
SW	−0.91533[a]
W	−0.51793[a]
NW	−0.25089[a]

[a] *P*-value is significant at 0.05 or lower.

Douglas-fir mortality was a result of beetle activity due to the sharp decline in NDMI after 2004 (Fig. 9). This trajectory is evident of rapid mortality, as opposed to more gradual spectral changes associated with defoliator species (Vogelmann et al., 2009). Whereas fire, blowdown or defoliation events have been documented as initiating Douglas-fir beetle outbreaks (Negrón et al., 2014), this is the first time that a landscape-scale outbreak has been associated with extreme drought. Douglas-fir stands in the study area are small and isolated, yet our methodology was successful at detecting the decline of these patches of forest. Finally, the decrease in NDMI of this stand several years after the drought (Fig. 9) is also indicative of mortality induced by beetles, compared to a deciduous stand (Fig. 10) where mortality was likely induced by the drought and not secondary agents. The temporal trajectory of NDMI in a declining coniferous stand (Fig. 9) is markedly different than the trajectory of a coniferous stand that was largely unaffected by the drought events (Fig. 12).

Subalpine fir decline has been attributed to mortality in fir forests in Colorado (Ciesla, 2010). Tree mortality is due to a combination of western balsam bark beetle (*Dryocoetes confuses*) (Meddens et al., 2012) and at least two species of fungi, *Armillaria* spp. and *Heterobasidium annosum*, known to cause root decay (Bigler et al., 2007; Ciesla, 2010). However, subalpine fir decline does not occur in large distinct patches common with other agents of conifer mortality, but rather heightened levels of background mortality. This particular type of mortality is more challenging to detect because it is not as conspicuous to human observers or readily detected with short time periods of satellite data (<5 years). Subalpine fir is the dominant conifer species on Little and Pine Mountains and significant negative trends were identified in these stands (Fig. 7). Mortality in subalpine fir forests has not been studied as extensively as other coniferous species and is a future research need. Spruce beetle (*Dendroctonus rufipennis*) is an important disturbance agent in Spruce-Fir forests, however the primary host, Engelmann Spruce (*Picea engelmannii*), is not commonly found in the study area. Western spruce budworm is also known to cause damage and mortality to subalpine fir by defoliation (Ciesla, 2010). We found a significantly higher percentage of mortality in large trees, which also suggests insect agents are a primary cause of mortality in the study area (Fig. 4a).

The primary deciduous tree in the study area, aspen, are susceptible to drought and a number of factors that can amplify or prolong the impact of moisture stress and lead to reduction in growth, partial dieback and mortality (Worrall et al., 2013). Factors include multi-year defoliation by tent caterpillars (*Malacosoma* spp.) and stem damage by fungi and insects which can kill the cambium and interrupt phloem, which leads to crown dieback (Worrall et al., 2013). We know of no documented defoliation events in our study area, but evidence of fungi (cankers) and insects (borers on standing dead and down trees) along with crown dieback were documented at over half of the sites in our study area. Furthermore, many trees had evidence of mechanical stem damage caused by elk. Late spring frost and freeze/thaw cycles during winter dormancy can also damage leaves and previous year's growth (Worrall et al., 2013). Without prior documentation of mortality agents, trend analysis can identify changes associated with drought over time and space in the study area. For example, the NDMI values for the aspen plots depicted in Figs. 10 and 12 prior to 2000 fluctuate between 0.2 and 0.4. However, after the start of the dry period in 2000 (Fig. 3), the NDMI of the plot in Fig. 10 drops below 0.2 and has not yet recovered (time example). Conversely, the NDMI of the plot in Fig. 12 has remained relatively constant after 2000. In this way, the temporal trends of individual pixels or plots can be explored to identify changes across space.

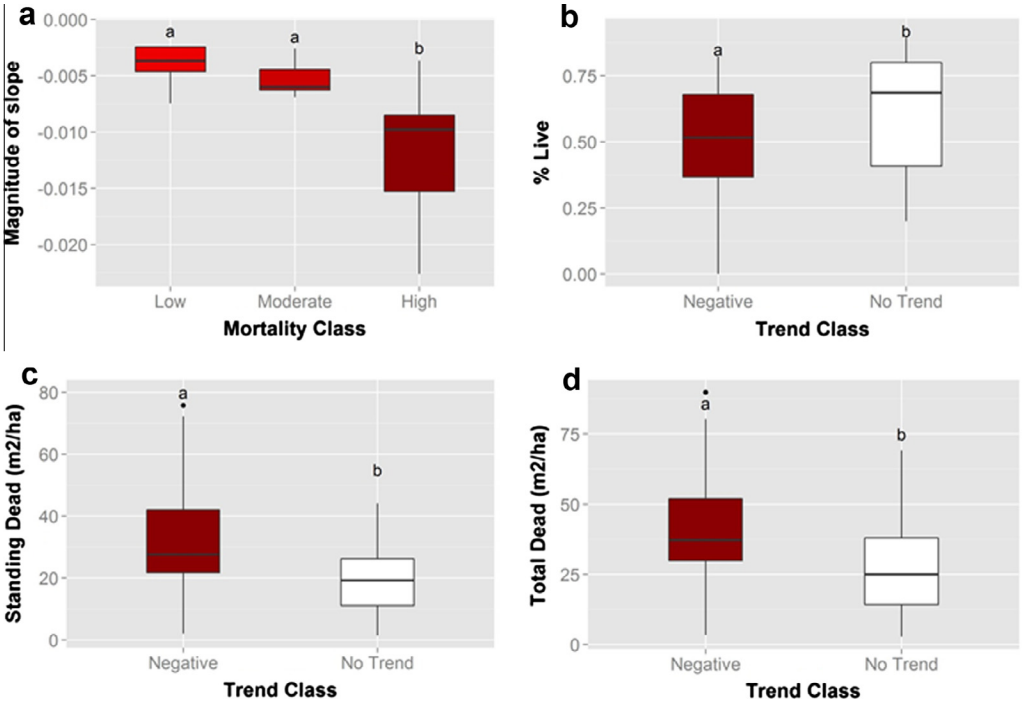

Fig. 8. (a) Boxplot of the variation in magnitude of slope for significant negative trends categorized by relative mortality of field plots (p-value < 0.05). (b) Boxplot of the variation of percent live trees between negative and no trend plots (p-value < 0.1). (c) Boxplot of the variation in basal area of standing dead trees for plots with negative and no trend (p-value < 0.05). (d) Boxplot of the variation in basal area of total dead trees (standing dead + down trees) for plots with negative and no trend (p-value < 0.05).

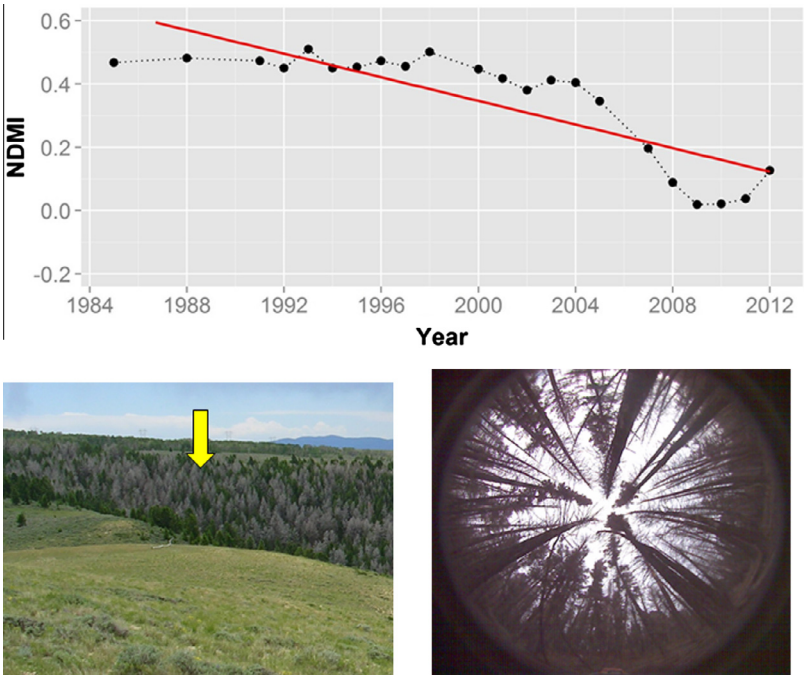

Fig. 9. Negative NDMI trend (p-value < 0.05) (top) of a field plot located in coniferous forest with high levels of mortality (bottom left; arrow is approximate location of plot). A hemispheric photo from the site indicates low plant area index and high canopy gap fraction (bottom right). Note, the hemispheric photo is one of nine photos at each plot (Fig. 2) used to calculate plant area index and canopy gap fraction. Photographs were taken by T. Assal.

Throughout the study area, we found a significantly higher percentage of mortality in small and medium aspen trees, compared to large trees (Fig. 4b). Given these findings, we suggest that there is cause for concern over the future of aspen forests in this area and represents a future research need.

4.2. Relationship between forest change trends and topography

We documented substantial levels of plot level mortality across forest type (Fig. 4) and identified negative trends throughout the study area (Fig. 7) using long-term satellite data. Although the

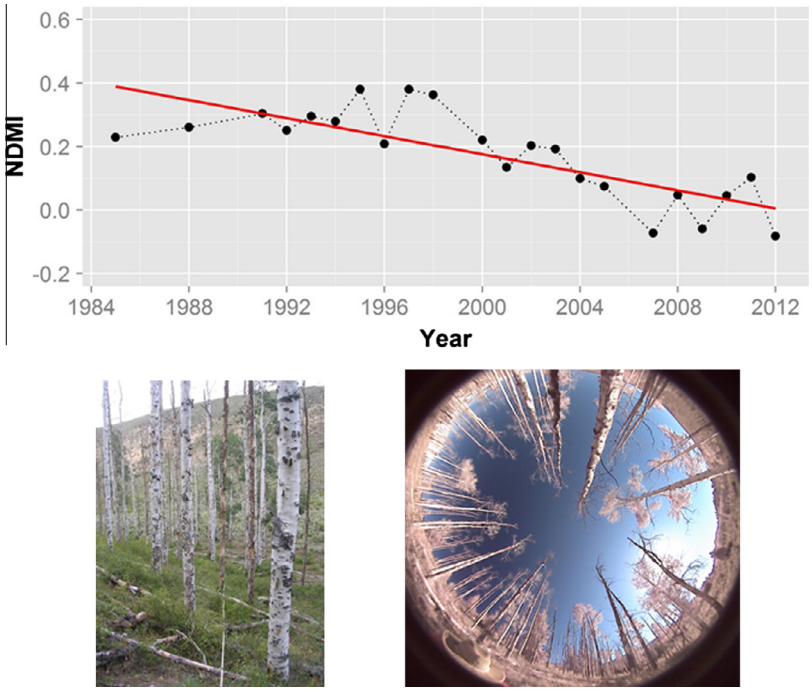

Fig. 10. Negative NDMI trend (p-value < 0.05) (top) of a field plot located in an open aspen stand with high levels of mortality (bottom left). A hemispheric photo from the site indicates very low plant area index and high canopy gap fraction (bottom right). Photographs were taken by T. Assal.

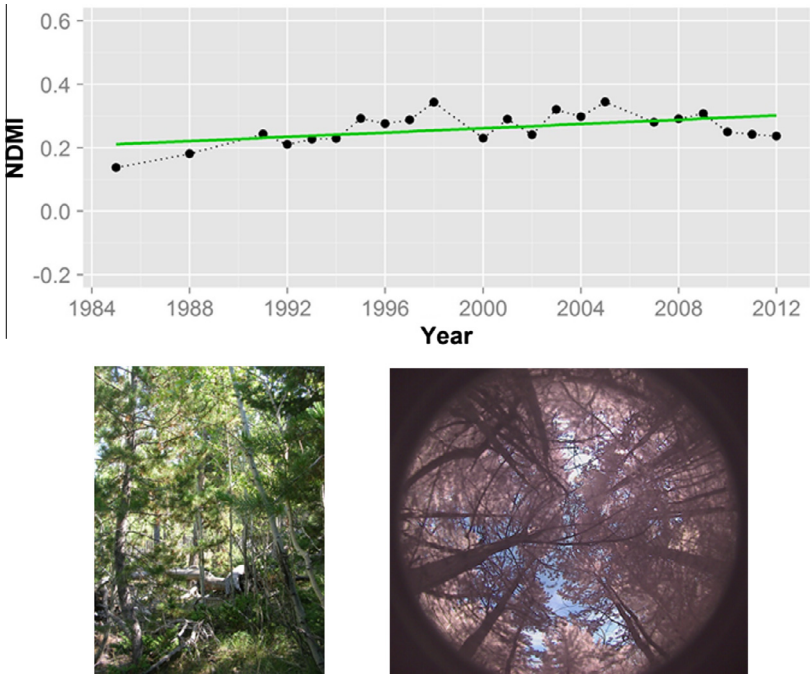

Fig. 11. Positive NDMI trend (p-value < 0.05) (top) of a field plot located in a dense coniferous forest with low levels of mortality (bottom left). A hemispheric photo from the site indicates high plant area index and low canopy gap fraction (bottom right). Photographs were taken by T. Assal.

physiology of drought-induced tree mortality is complex (McDowell et al., 2008), an understanding of the spatial pattern of tree decline is an important consideration for managers. Mechanistic studies of drought impacts on tree physiology is an emerging research trend and out of the scope of our study. However, our results serve as a coarse filter to highlight areas of mortality or significant forest change where mechanistic studies could be initiated (Huang and Anderegg, 2012).

The aspect of a slope has direct influence on incident solar radiation and surface temperature (McCune and Keon, 2002) and indirectly influences evaporation and available soil moisture (Huang and Anderegg, 2012). Studies that evaluated acute drought-induced mortality in other Rocky Mountain aspen forests found higher mortality rates on drier southern and western aspects (Huang and Anderegg, 2012; Worrall et al., 2008). However, our results contrast with these studies as we found higher than

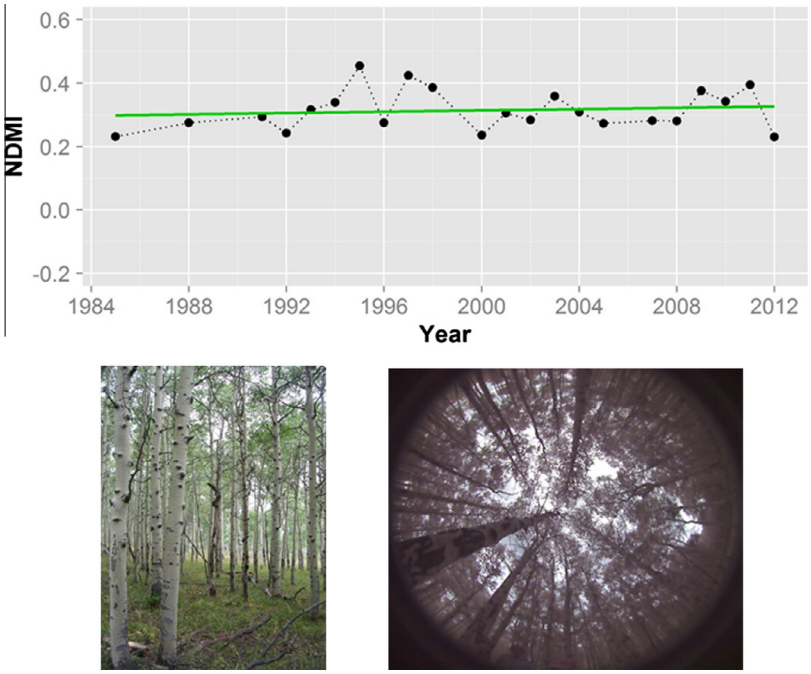

Fig. 12. Stable NDMI trend (p-value not significant) (top) of a field plot located in aspen forest with low levels of mortality (bottom right). A hemispheric photo from the site indicates high plant area index and low canopy gap fraction (bottom left). Photographs were taken by T. Assal.

expected rates of negative trends of deciduous and coniferous trees on north aspects (Table 5). This indicates the aspen forests in our study area are very different than aspen forests in other parts of the intermountain west. Genetic research suggests that aspen clones exhibit wide-ranging phenotypic variation in physiology and growth traits under drought conditions (St. Clair et al., 2010). Localized mortality of aspen could be due to genotype (clonal) effects (Huang and Anderegg, 2012), and adaptation could also explain regional differences in spatial patterns of decline.

We do not know when the aspen genets (clones) were established in our study area, but conditions were presumably wetter for some period conducive to establishment. Our study area has likely always been drier than other Rocky Mountain forests for some time and as a result, these genets might be more adapted to arid conditions. We found higher elevations and northern aspects most likely to exhibit significant negative trends. These areas are cooler and wetter than other aspects, and trees would be most vulnerable in these areas in years when winter precipitation is below average. The density of trees on northern slopes could have increased during the wet decade of the 1990s (Fig. 3), setting up those same slopes for an increase in mortality when water was limited during drought years. Although we documented substantial mortality and areas of negative trends, we did not observe large scale mortality documented by others (Huang and Anderegg, 2012; Worrall et al., 2008). This highlights the value of spatially explicit analysis and the importance of landscape position in arid landscapes.

4.3. Management implications

Regional climate exerts top-down control on ecosystems (Stephenson, 1990) and is an important consideration for managers when considering the future outlook of an ecosystem or treatment options. The current climate profiles for many of the tree species analyzed in this study are predicted to no longer be present in the isolated forests of the study area as we approach the next century (Crookston et al., 2010; Rehfeldt et al., 2009). However, many global and regional climate models do not currently take terrain into account (Crookston et al., 2010). Our study provides spatially explicit evidence that bottom-up controls, including fine-scale topography, remain important in climatically driven drought (Prichard and Kennedy, 2014). Adaptive management could benefit from spatially explicit analysis and data because aspen forests do not function the same across locations (Rogers et al., 2014) or within the confines of coarse scale data used in climate models. The results of our analysis can frame hypotheses to be tested with regard to resistance, persistence or vulnerability of forests to drought. Resistance is the capacity of an ecosystem to remain largely unchanged, with regard to structure, processes and functioning, despite stresses and disturbance (Folke et al., 2004). We suggest areas with a significant positive trend are resistant to drought episodes of these magnitudes. These areas had a statistically significant increase in canopy moisture despite several recent extreme droughts (e.g. 2002, 2012) and an extended dry period (e.g. 2000–2004). These forests likely increased in structural, functional, and physiological capacity during this time period which resulted in increased productivity, such as the plot in Fig. 11. Forests that did not have a statistically significant trend in either direction can be considered persistent during periods punctuated by drought. For example, the aspen stand depicted in Fig. 12 has maintained persistent NDMI values over the last 25 years. Finally, areas with a significant negative trend are vulnerable to drought. The structural, functional and physiological properties of these stands markedly declined after these events, and in some areas resulted in substantial mortality (Figs. 9 and 10). Our framework provides information on change over time at local scales (e.g. pixel or stand level) (Figs. 9–12). We believe the results of our study can benefit managers in utilizing limited budgets to ensure the long-term persistence of aspen forest in this area.

4.4. Ecological and technical considerations

We suggest that several spatial and temporal characteristics of the forest-shrubland ecotone be taken into consideration with our

approach as quantifying tree canopy dynamics through remote sensing in these areas remains a challenge (Yang et al., 2012). Coniferous forests have a closed architecture which enables robust modeling using remotely sensed data (Assal et al., 2015). However, semi-arid aspen systems found at lower elevations in our study area present challenges to evaluate gradual dynamics over time. These systems tend to have low tree cover and density, a very open canopy and low values of plant area index. Furthermore, the combination of trees, shrubs and grasses may confound the spectral signal as pixel values are a mixture of ground elements (Lefsky and Cohen, 2003). Shrublands have lower values of NDMI compared to forested pixels, therefore trends in sparse aspen forest could be muted as shrubs dominate the spectral signal. Given the high heterogeneity between forest and non-forest present in our study area, mortality might be underestimated, particularly at the margins of forest patches. The hemispheric photos are an efficient and objective method to calculate plant area index and canopy gap fraction; however, there are differences in measurements between forest functional type. PAI tends to be skewed in plots dominated by large, dead conifer trees, compared to aspen dominated plots. For example, the PAI of the plot in Fig. 9 is much higher than the PAI in Fig. 10 (1.22–0.43), yet the live basal area is lower (8.39 m^2/ha to 12.8 m^2/ha). In addition, the live basal area of the aspen plot (Fig. 10) was skewed by several large trees where >75% of the canopy was dead and therefore not contributing the canopy moisture (NDMI). The time series would be more robust if we were able to obtain one image per year, but clouds, sensor issues, etc. limited available data. Numerious studies have utilized the rich temporal archive of MODIS data with daily to bi-weekly collections of imagery that can track both long-term and interannual phenology differences. However, the fine-scale heterogeneity of the study area and our interest to extend the study prior to 2000 prevented the use of MODIS data.

There are no long-term plots in the study area so we have no information on mortality rates. However, the results of our study suggest forest change (Fig. 6) may be linked with long-term trends in precipitation (Fig. 3) and long-term analysis is required to understand the cumulative effects of drought years in this ecosystem. Given the suggested mechanisms of mortality (Section 4.1), we suspect there has been a continuum of mortality triggered by severe drought and our long-term field data confirm this suspicion as some plots had trees at different stages of decomposition (e.g. standing dead trees with fine branches still present, down trees in early stages of decomposition, etc.). Stands with a high level of mortality over a short time period will have a relatively quick change in NDMI. These areas will likely have a heightened chance of detection due to rapid change in NDMI. However, areas that exhibit lower amounts of mortality over longer time periods will have a smaller change in NDMI over a longer time period. The advantage of the time series approach should capture both hypothetical examples that might be otherwise missed by a small number of time periods. Alternatively, piecewise linear models could be fit to the long-term data to analyze trends before and after a disturbance event. However, we stress caution with this method when using a limited number of Landsat observations as the timing of an image, combined with an enforced breakpoint, could identify spurious trends.

5. Conclusion

Forests in the southern portion of the Wyoming Basin ecoregion experienced a relatively dry decade punctuated by two years of extreme drought. However, little is known about the baseline condition of these forests, and how climate, in particular drought, affects this topographically complex ecosystem. We quantified the effects of multiple droughts on deciduous and coniferous forest at local scales using field data, satellite imagery and trend analysis. We identified an appropriate vegetation index (NDMI) that best represented short-term forest conditions (e.g. plant area index and canopy gap fraction) of the study area. We applied the index to a 22-year Landsat time series to identify the location, direction and magnitude of forest change by forest cover type. We used field data to correlate long-term spectral trends to changes in demographic, structural, functional, and physiological properties of deciduous and coniferous forest. Mortality was greatest in the largest size class of coniferous trees, but we found a higher percentage of mortality in small and medium aspen trees, which has important implications for the future of these forests. Nearly half of the field plots had a significant negative trend between 1985 and 2012, and those plots also had a significantly higher amount of standing dead and down trees compared to plots with no trend. Forests on north aspects were most likely to exhibit significant negative trends in this topographically complex landscape.

Our analysis provides managers with a long-term perspective of the forest dynamics of this ecosystem with respect to variability in precipitation. The field data provide evidence and demonstrate application of assessing long-term trends with Landsat imagery at fine spatial scales in a forest-shrubland matrix. We believe our study is the first to retrospectively document a largescale Douglas-fir beetle outbreak that was initiated by extreme drought, as opposed to fire, blowdown or a defoliation event. Our methodology is well suited to identify subalpine fir decline, which unlike other agents of conifer mortality, results in heightened levels of background mortality over large areas. Due to this mechanism of mortality, subalpine fir decline has rarely been documented outside of aerial detection surveys and this study. We believe the methodology and results of this assessment provide a valuable perspective to resource managers and highlights potential opportunities to work across jurisdictional lines. Our results identify areas of forest that are resistant, persistent or vulnerable to severe drought. The framework relies heavily on open access satellite data and could be applied to long-term monitoring of similar ecosystems.

Acknowledgements

This research was supported by the USGS Fort Collins Science Center and the Wyoming Landscape Conservation Initiative. Logistical support was provided by the Wyoming Game and Fish Department and Bureau of Land Management Rock Springs Field Office. We gratefully acknowledge two anonymous reviewers for their comments that helped to improve the manuscript. We thank Zachary Bowen, Geneva Chong, Daniel Manier, Alexandra Urza, and Marie Dematatis for discussion on research direction and/or assistance in collection of field data and Anne and Jim Assal for their contributions to data entry.

Any use of trade, firm, or product names is for descriptive purposes only and does not imply endorsement by the U.S. Government.

References

Abbas, S., Nichol, J.E., Qamer, F.M., Xu, J., 2014. Characterization of drought development through remote sensing: a case study in Central Yunnan, China. Remote Sens. 6, 4998–5018.

Agnew, C.T., 2000. Using the SPI to identify drought. Drought Netw. News 12, 6–12.

Allen, C.D., Breshears, D.D., 1998. Drought-induced shift of a forest-woodland ecotone: rapid landscape response to climate variation. Proc. Natl. Acad. Sci. 95, 14839–14842.

Allen, C.D., Macalady, A.K., Chenchouni, H., Bachelet, D., McDowell, N., Vennetier, M., Kitzberger, T., Rigling, A., Breshears, D.D., Hogg, E.H. (Ted), Gonzalez, P., Fensham, R., Zhang, Z., Castro, J., Demidova, N., Lim, J.-H., Allard, G., Running, S. W., Semerci, A., Cobb, N., 2010. A global overview of drought and heat-induced

tree mortality reveals emerging climate change risks for forests. For. Ecol. Manage. 259, 660–684. http://dx.doi.org/10.1016/j.foreco.2009.09.001.
Assal, T.J., Anderson, P., Sibold, J., 2015. Mapping forest functional type in a forest-shrubland ecotone using SPOT imagery and predictive habitat distribution modelling. Remote Sens. Lett. 6, 755–764. http://dx.doi.org/10.1080/2150704X.2015.1072289.
Assal, T.J., Sibold, J., Reich, R., 2014. Modeling a historical mountain pine beetle outbreak using Landsat MSS and multiple lines of evidence. Remote Sens. Environ. 155, 275–288. http://dx.doi.org/10.1016/j.rse.2014.09.002.
Baguskas, S.A., Peterson, S.H., Bookhagen, B., Still, C.J., 2014. Evaluating spatial patterns of drought-induced tree mortality in a coastal California pine forest. For. Ecol. Manage. 315, 43–53. http://dx.doi.org/10.1016/j.foreco.2013.12.020.
Bastos, A., Gouveia, C.M., Trigo, R.M., Running, S.W., 2014. Analysing the spatio-temporal impacts of the 2003 and 2010 extreme heatwaves on plant productivity in Europe. Biogeosciences 11, 3421–3435. http://dx.doi.org/10.5194/bg-11-3421-2014.
Bentz, B.J., Régnière, J., Fettig, C.J., Hansen, E.M., Hayes, J.L., Hicke, J.A., Kelsey, R.G., Negrón, J.F., Seybold, S.J., 2010. Climate change and bark beetles of the Western United States and Canada: direct and indirect effects. Bioscience 60, 602–613. http://dx.doi.org/10.1525/bio.2010.60.8.6.
Bigler, C., Gavin, D.G., Gunning, C., Veblen, T.T., 2007. Drought induces lagged tree mortality in a subalpine forest in the Rocky Mountains. Oikos 116, 1983–1994. http://dx.doi.org/10.1111/j.2007.0030-1299.16034.x.
Breshears, D.D., Cobb, N., Rich, P.M., Price, K.P., Allen, C.D., Balice, R.G., Romme, W.H., Kastens, J.H., Floyd, M.L., Belnap, J., Anderson, J.J., Myers, O.B., Meyer, C.W., 2005. Regional vegetation die-off in response to global-change-type drought. Proc. Natl. Acad. Sci. USA 102, 15144–15148. http://dx.doi.org/10.1073/pnas.0505734102.
Campbell, G.S., Norman, J.M., 1989. The description and measurement of plant canopy structure. In: Russell, G., Marshall, B., Jarvis, P.G. (Eds.), Plant Canopies: Their Growth, Form, and Function, Society for Experimental Biology: 31. Cambridge University Press, Cambridge, United Kingdom, pp. 1–19.
Carreiras, J.M.B., Pereira, J.M.C., Pereira, J.S., 2006. Estimation of tree canopy cover in evergreen oak woodlands using remote sensing. For. Ecol. Manage. 223, 45–53. http://dx.doi.org/10.1016/j.foreco.2005.10.056.
Chander, G., Markham, B.L., Helder, D.L., 2009. Remote Sensing of Environment Summary of current radiometric calibration coefficients for Landsat MSS, TM, ETM+, and EO-1 ALI sensors. Remote Sens. Environ. 113, 893–903. http://dx.doi.org/10.1016/j.rse.2009.01.007.
Ciesla, W.M., 2010. 2010 Report on the Health of Colorado's Forests. Fort Collins, CO.
Cook, E.R., Woodhouse, C.A., Eakin, C.M., Meko, D.M., Stahle, D.W., 2004. Long-term aridity changes in the western United States. Science 306, 1015–1018. http://dx.doi.org/10.1126/science.1102586.
Crookston, N.L., Rehfeldt, G.E., Dixon, G.E., Weiskittel, A.R., 2010. Addressing climate change in the forest vegetation simulator to assess impacts on landscape forest dynamics. For. Ecol. Manage. 260, 1198–1211. http://dx.doi.org/10.1016/j.foreco.2010.07.013.
Czerwinski, C.J., King, D.J., Mitchell, S.W., 2014. Mapping forest growth and decline in a temperate mixed forest using temporal trend analysis of Landsat imagery, 1987–2010. Remote Sens. Environ. 141, 188–200. http://dx.doi.org/10.1016/j.rse.2013.11.006.
DeRose, R.J., Long, J.N., Ramsey, R.D., 2011. Combining dendrochronological data and the disturbance index to assess Engelmann spruce mortality caused by a spruce beetle outbreak in southern Utah, USA. Remote Sens. Environ. 115, 2342–2349. http://dx.doi.org/10.1016/j.rse.2011.04.034.
Deshayes, M., Guyon, D., Jeanjean, H., Stach, N., Jolly, A., Hagolle, O., 2006. The contribution of remote sensing to the assessment of drought effects in forest ecosystems. Ann. For. Sci. 63, 579–595. http://dx.doi.org/10.1051/forest.
Dobrowski, S.Z., 2011. A climatic basis for microrefugia: the influence of terrain on climate. Glob. Change Biol. 17, 1022–1035. http://dx.doi.org/10.1111/j.1365-2486.2010.02263.x.
Dorman, M., Svoray, T., Perevolotsky, A., Sarris, D., 2013. Forest performance during two consecutive drought periods: diverging long-term trends and short-term responses along a climatic gradient. For. Ecol. Manage. 310, 1–9.
Eidenshink, J., Schwind, B., Brewer, K., Zhu, Z.-L., Quayle, B., Howard, S., 2007. A project for monitoring trends in burn severity. Fire Ecol. 3, 3–21.
Folke, C., Carpenter, S., Walker, B., Scheffer, M., Elmqvist, T., Gunderson, L., Holling, C.S., 2004. Regime shifts, resilience, and biodiversity in ecosystem management. Annu. Rev. Ecol. Evol. Syst. 35, 557–581. http://dx.doi.org/10.1146/annurev.ecolsys.35.021103.105711.
Foster, D.R., Knight, D.H., Franklin, J.F., 1998. Landscape patterns and legacies resulting from large, infrequent forest disturbances. Ecosystems 1, 497–510. http://dx.doi.org/10.1007/s100219900046.
Gitlin, A.R., Sthultz, C.M., Bowker, M.A., Stumpf, S., Paxton, K.L., Kennedy, K., Muñoz, A., Bailey, J.K., Whitham, T.G., 2006. Mortality gradients within and among dominant plant populations as barometers of ecosystem change during extreme drought. Conserv. Biol. 20, 1477–1486. http://dx.doi.org/10.1111/j.1523-1739.2006.00424.x.
Goodwin, N.R., Coops, N.C., Wulder, M.A., Gillanders, S., Schroeder, T.A., Nelson, T., 2008. Estimation of insect infestation dynamics using a temporal sequence of Landsat data. Remote Sens. Environ. 112, 3680–3689. http://dx.doi.org/10.1016/j.rse.2008.05.005.
Gosz, J.R., 1992. Gradient analysis of ecological change in time and space: implications for forest management. Ecol. Appl. 2, 248–261.
Hardisky, M.A., Klemas, V., Smart, R.M., 1983. The influence of soil salinity, growth form, and leaf moisture on the spectral radiance of Spartina alterniflora canopies. Photogramm. Eng. Remote Sens. 49, 77–83.
Hessl, A.E., Graumlich, L.J., 2002. Interactive effects of human activities, herbivory and fire on quaking aspen (Populus tremuloides) age structures in western Wyoming. J. Biogeogr. 29, 889–902. http://dx.doi.org/10.1046/j.1365-2699.2002.00703.x.
Hogg, E.H., Brandt, J.P., Michaelian, M., 2008. Impacts of a regional drought on the productivity, dieback, and biomass of western Canadian aspen forests. Can. J. For. Res. 38, 1373–1384. http://dx.doi.org/10.1139/X08-001.
Hogg, E.H., Saugier, B., Pontailler, J.Y., Black, T.A., Chen, W., Hurdle, P.A., Wu, A., 2000. Responses of trembling aspen and hazelnut to vapor pressure deficit in a boreal deciduous forest. Tree Physiol. 20, 725–734.
Hope, A., Fouad, G., Granovskaya, Y., 2014. Evaluating drought response of Southern Cape Indigenous Forests, South Africa, using MODIS data. Int. J. Remote Sens. 35, 4852–4864. http://dx.doi.org/10.1080/01431161.2014.930205.
Huang, C.Y., Anderegg, W.R.L., 2012. Large drought-induced aboveground live biomass losses in southern Rocky Mountain aspen forests. Glob. Change Biol. 18, 1016–1027. http://dx.doi.org/10.1111/j.1365-2486.2011.02592.x.
Huete, A., Didan, K., Miura, T., Rodriguez, E.P., Gao, X., Ferreira, L.G., 2002. Overview of the radiometric and biophysical performance of the MODIS vegetation indices. Remote Sens. Environ. 83, 195–213. http://dx.doi.org/10.1016/S0034-4257(02)00096-2.
Huete, A.R., 1988. A soil-adjusted vegetation index (SAVI). Remote Sens. Environ. 25, 295–309.
Jones, H.G., Vaughan, R.H., 2010. Remote Sensing of Vegetation: Principles, Techniques, and Applications. Oxford University Press, Oxford, UK.
Kennedy, R.E., Yang, Z., Cohen, W.B., 2010. Detecting trends in forest disturbance and recovery using yearly Landsat time series: 1. LandTrendr—Temporal segmentation algorithms. Remote Sens. Environ. 114, 2897–2910. http://dx.doi.org/10.1016/j.rse.2010.07.008.
Knight, D.H., 1994. Mountains and Plains: The Ecology of Wyoming Landscapes. Yale University, New Haven, CT.
Kulakowski, D., Kaye, M.W., Kashian, D.M., 2013. Long-term aspen cover change in the western US. For. Ecol. Manage. 299, 52–59. http://dx.doi.org/10.1016/j.foreco.2013.01.004.
Lefsky, M., Cohen, W., 2003. Selection of remotely sensed data. In: Wulder, M.A., Franklin, S. (Eds.), Remote Sensing of Forest Environments: Concepts and Case Studies. Kluwer Academic Publishers, Boston, pp. 13–47.
Littell, J.S., McKenzie, D., Peterson, D.L., Westerling, A.L., 2009. Climate and wildfire area burned in western U.S. ecoprovinces, 1916–2003. Ecol. Appl. 19, 1003–1021.
Lloret, F., Lobo, a., Estevan, H., Maisongrande, P., Vayreda, J., Terradas, J., 2007. Woody plant richness and NDVI response to drought events in Catalonian (northeastern Spain) forests. Ecology 88, 2270–2279.
Martens, S.N., Ustin, S.L., Rousseau, R.A., 1993. Estimation of tree canopy leaf area index by gap fraction analysis. For. Ecol. Manage. 61, 91–108.
Masek, J., Vermote, E.F., Saleous, N.E., Wolfe, R., Hall, F.G., Huemmrich, K.F., Gao, F., Kutler, J., Lim, T., 2006. A Landsat surface reflectance dataset. IEEE Geosci. Remote Sens. Lett. 3, 68–72. http://dx.doi.org/10.1109/LGRS.2005.857030.
Maselli, F., 2004. Monitoring forest conditions in a protected Mediterranean coastal area by the analysis of multiyear NDVI data. Remote Sens. Environ. 89, 423–433. http://dx.doi.org/10.1016/j.rse.2003.10.020.
McCune, B., Keon, D., 2002. Equations for potential annual direct incident radiation and heat load. J. Veg. Sci. 13, 603–606.
McDowell, N., Pockman, W.T., Allen, C.D., Breshears, D.D., Cobb, N., Kolb, T., Plaut, J., Sperry, J., West, A., Williams, D.G., Yepez, E.a., 2008. Mechanisms of plant survival and mortality during drought: why do some plants survive while others succumb to drought? New Phytol. 178, 719–739. http://dx.doi.org/10.1111/j.1469-8137.2008.02436.x.
McManus, K.M., Morton, D.C., Masek, J.G., Wang, D., Sexton, J.O., Nagol, J.R., Ropars, P., Boudreau, S., 2012. Satellite-based evidence for shrub and graminoid tundra expansion in northern Quebec from 1986 to 2010. Glob. Change Biol. 18, 2313–2323. http://dx.doi.org/10.1111/j.1365-2486.2012.02708.x.
Meddens, A.J.H., Hicke, J.A., Ferguson, C.A., 2012. Spatiotemporal patterns of observed bark beetle-caused tree mortality in British Columbia and the western United States. Ecol. Appl. 22, 1876–1891.
Meddens, A.J.H., Hicke, J.A., Vierling, L.A., Hudak, A.T., 2013. Evaluating methods to detect bark beetle-caused tree mortality using single-date and multi-date Landsat imagery. Remote Sens. Environ. 132, 49–58. http://dx.doi.org/10.1016/j.rse.2013.01.002.
Meigs, G.W., Kennedy, R.E., Cohen, W.B., 2011. A Landsat time series approach to characterize bark beetle and defoliator impacts on tree mortality and surface fuels in conifer forests. Remote Sens. Environ. 115, 3707–3718. http://dx.doi.org/10.1016/j.rse.2011.09.009.
Michaelian, M., Hogg, E.H., Hall, R.J., Arsenault, E., 2011. Massive mortality of aspen following severe drought along the southern edge of the Canadian boreal forest. Glob. Change Biol. 17, 2084–2094. http://dx.doi.org/10.1111/j.1365-2486.2010.02357.x.
Negrón, J., Lynch, A., Schaupp, W., Mercado, J., 2014. Douglas-fir tussock moth- and Douglas-fir beetle-caused mortality in a ponderosa Pine/Douglas-fir forest in the Colorado Front Range, USA. Forests 5, 3131–3146. http://dx.doi.org/10.3390/f5123131.
NEON, 2000. Report on first Workshop on the National Ecological Observatory Network (NEON). Lake Placid, Florida.

NOAA, 2012. NOAA National Climatic Data Center, State of the Climate: Drought for September 2012 [WWW Document]. State Clim. URL <http://www.ncdc.noaa.gov/sotc/drought/201209> (accessed 05.25.15).

Pfeifer, M., Gonsamo, A., Disney, M., Pellikka, P., Marchant, R., 2012. Leaf area index for biomes of the Eastern Arc Mountains: Landsat and SPOT observations along precipitation and altitude gradients. Remote Sens. Environ. 118, 103–115. http://dx.doi.org/10.1016/j.rse.2011.11.009.

Prichard, S.J., Kennedy, M.C., 2014. Fuel treatments and landform modify landscape patterns of burn severity in an extreme fire event. Ecol. Appl. 24, 571–590.

Rehfeldt, G.E., Ferguson, D.E., Crookston, N.L., 2009. Aspen, climate, and sudden decline in western USA. For. Ecol. Manage. 258, 2353–2364. http://dx.doi.org/10.1016/j.foreco.2009.06.005.

Rogers, P.C., Landhausser, S.M., Pinno, B.D., Ryel, R.J., 2014. A functional framework for improved management of Western North American Aspen (Populus tremuloides Michx.). For. Manag. 60, 345–359.

Rousse, J.W., Hass, R.H., Schell, J.A., Deering, D.W., Harlan, J.C., 1974. Monitoring the Vernal Advancement of Retrogradation of Natural Vegetation, Type III, Final Report. Greenbelt, Maryland.

Sousa, W.P., 1984. The role of disturbance in natural communities. Annu. Rev. Ecol. Syst. 15, 353–391.

St. Clair, S.B., Mock, K.E., LaMalfa, E.M., Campbell, R.B., Ryel, R.J., 2010. Genetic contributions to phenotypic variation in physiology, growth, and vigor of western aspen (Populus tremuloides) clones. For. Sci. 56, 222–230 (doi: none).

Stephenson, N.L., 1990. Climatic control of vegetation distribution: the role of the water balance. Am. Nat. 135, 649–670.

Thornthwaite, C., 1953. A charter for climatology. World Meteorol. Organ. Bull. 2, 40–46.

Turner, M.G., Baker, W.L., Peterson, C.J., Peet, R.K., 1998. Factors influencing succession: lessons from large, infrequent natural disturbances. Ecosystems, 511–523.

Turner, M.G., Dale, V.H., 1998. Comparing large, infrequent disturbances: what have we learned? Ecosystems 1, 493–496.

Tüshaus, J., Dubovyk, O., Khamzina, A., Menz, G., 2014. Comparison of medium spatial resolution ENVISAT-MERIS and Terra-MODIS time series for vegetation decline analysis: a case study in Central Asia. Remote Sens. 6, 5238–5256. http://dx.doi.org/10.3390/rs6065238.

USGS, 2014. EarthExplorer archive [WWW Document]. URL <http://edcsns17.cr.usgs.gov/NewEarthExplorer/>.

Van Mantgem, P.J., Stephenson, N.L., Byrne, J.C., Daniels, L.D., Franklin, J.F., Fulé, P.Z., Harmon, M.E., Larson, A.J., Smith, J.M., Taylor, A.H., Veblen, T.T., 2009. Widespread increase of tree mortality rates in the western United States. Science 323 (80), 521–524. http://dx.doi.org/10.1126/science.1165000.

Vicente-Serrano, S.M., 2007. Evaluating the impact of drought using remote sensing in a Mediterranean, Semi-arid Region. Nat. Hazards 40, 173–208. http://dx.doi.org/10.1007/s11069-006-0009-7.

Vogelmann, J.E., Tolk, B., Zhu, Z., 2009. Monitoring forest changes in the southwestern United States using multitemporal Landsat data. Remote Sens. Environ. 113, 1739–1748. http://dx.doi.org/10.1016/j.rse.2009.04.014.

Vogelmann, J.E., Xian, G., Homer, C., Tolk, B., 2012. Monitoring gradual ecosystem change using Landsat time series analyses: Case studies in selected forest and rangeland ecosystems. Remote Sens. Environ. 122, 92–105. http://dx.doi.org/10.1016/j.rse.2011.06.027.

Volcani, A., Karnieli, A., Svoray, T., 2005. The use of remote sensing and GIS for spatio-temporal analysis of the physiological state of a semi-arid forest with respect to drought years. For. Ecol. Manage. 215, 239–250. http://dx.doi.org/10.1016/j.foreco.2005.05.063.

Weiss, J.L., Gutzler, D.S., Allred, J.E., Dahm, C.N., 2004. Long-term vegetation monitoring with NDVI in a diverse semi-arid setting, central New Mexico, USA. J. Arid Environ. 58, 249–272. http://dx.doi.org/10.1016/j.jaridenv.2003.07.001.

Westerling, A.L., Hidalgo, H.G., Cayan, D.R., Swetnam, T.W., 2006. Warming and earlier spring increase western U.S. forest wildfire activity. Science 313 (80), 940–943. http://dx.doi.org/10.1126/science.1128834.

Wilson, E.H., Sader, S.A., 2002. Detection of forest harvest type using multiple dates of Landsat TM imagery. Remote Sens. Environ. 80, 385–396. http://dx.doi.org/10.1016/S0034-4257(01)00318-2.

Worrall, J.J., Egeland, L., Eager, T., Mask, R.A., Johnson, E.W., Kemp, P.A., Shepperd, W.D., 2008. Rapid mortality of Populus tremuloides in southwestern Colorado, USA. For. Ecol. Manage. 255, 686–696. http://dx.doi.org/10.1016/j.foreco.2007.09.071.

Worrall, J.J., Rehfeldt, G.E., Hamann, A., Hogg, E.H., Marchetti, S.B., Michaelian, M., Gray, L.K., 2013. Recent declines of Populus tremuloides in North America linked to climate. For. Ecol. Manage. 299, 35–51. http://dx.doi.org/10.1016/j.foreco.2012.12.033.

Yang, J., Weisberg, P.J., Bristow, N.A., 2012. Landsat remote sensing approaches for monitoring long-term tree cover dynamics in semi-arid woodlands: comparison of vegetation indices and spectral mixture analysis. Remote Sens. Environ. 119, 62–71. http://dx.doi.org/10.1016/j.rse.2011.12.004.